THE BIRD-CAGE METHOD USED FOR MEASURING CYLINDRICITY. A PROBLEM OF OPTIMAL PROFILE MATCHING.

Dariusz Janecki [1], *Jarosław Zwierzchowski* [2]

[1] Kielce University of Technology, Kielce, Poland, djanecki@tu.kielce.pl
[2] Kielce University of Technology, Kielce, Poland, j.zwierzchowski@tu.kielce.pl

Abstract − The bird-cage method used for measuring cylindricity is reported to be the most effective, as it provides the most detailed information about an analyzed object. The average values of profiles measured with the cross-section and the generatrix methods may differ slightly, yet this may result from some design imperfections of the measurement instruments used. In this study, the problem of optimal profile matching is formulated and solved. As a result, the differences between the values of the registered profiles at the points of intersection of the scanning trajectories can be minimized.

Keywords: cylindricity, bird-cage method, profile matching

1. INTRODUCTION

Rotary components constitute a large and important group of machine parts. They are common, for instance, in the automotive, power, paper and shipbuilding industries; therefore, one of the most significant metrological tasks today is to ensure maximum accuracy of roundness and cylindricity measurements [1-7].

Cylindrically shaped objects have generally been assessed by measuring their roundness deviations at several cross-sections. In practice, the reliability of a product is dependent on the whole area of the surface. It is desirable that cylindrical components be evaluated by means of the parameters that refer to the whole surface area.

Cylindricity needs to be measured in such a way that the representation of the measured surface is as precise as possible. It is important to ensure appropriate density of measuring points. The basic criterion for selecting a measurement method is to assume the predominant harmonic for both roundness and straightness profiles. In practice, it is difficult to cover the entire surface with measuring points using the theoretical minimum density of points defined in the ISO 12180 standard [8]. The standard describes the measurement methods that provide specific rather than general information about cylindrically shaped objects. These are: the cross-section method, the generatrix method, the bird-cage method being a combination of the previous two, and the point method. The first three methods are graphically illustrated in Fig. 1.

The cross-section and the generatrix methods are implemented in the majority of instruments applying the radial method. The point method is frequently employed when form deviations are assessed by means of coordinate measuring machines. The ISO 12180 standard recommends using the bird-cage method. Surprisingly, it is not commonly used to measure cylindricity deviations even though it provides the most detailed information about measured objects [9,10].

It appears that the average values of profiles measured with the cross-section and the generatrix methods differ slightly. This may be due to certain design imperfections of the measurement instruments used. In this study, the problem of optimal profile matching is formulated and solved. As a consequence, the differences between the values of the registered profiles at the points of intersection of the scanning trajectories can be minimized.
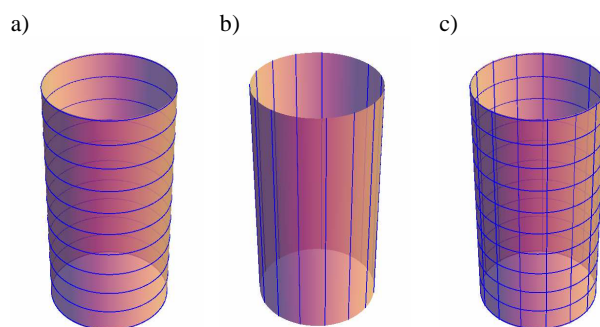
Fig.1. Cylindricity measurement methods recommended in the ISO 12180 standard [8]: a) the cross-section method, b) the generatrix method, c) the bird-cage method

2. METHODOLOGY

Let us consider an XYZ Cartesian coordinate system representing the measurement table where the Z-axis coincides with the spindle rotation axis. It is also convenient to apply a cylindrical coordinate system because the radial method of measurement of the macrogeometry of cylindrical surfaces involves scanning the object surface during the spindle rotation and the vertical shift of the sensor. The coordinates of a point in the cylindrical system associated with the XYZ system are represented by three numbers (φ, r, z), where φ is the angular coordinate of the point, r is the radial coordinate (distance of the point from the Z-axis), and z is the height-related coordinate. A cylindricity

profile can be written parametrically using the following function:

$$r_{cyl}(\varphi, z) \tag{1}$$

where

$$0 \leq \varphi \leq 2\pi \ \text{and} \ 0 \leq z \leq H \ . \tag{2}$$

The bird-cage method applied to measure the cylindricity of rotary objects combines the principles of the cross-section and the generatrix methods. It is assumed that the instrument is equipped with high precision systems for measuring the sensor height and the angle of table or spindle rotation.

When a profile is to be measured at a selected cross-section, the vertical shift of the sensor is switched off. The sensor needs to be shifted to a desired height and the table or spindle rotation switched on. The moment the control system receives a signal of the zero angular position, the measurement starts. It is assumed that the height coordinates of the consecutive cross-sections are: $z_n, n = 1,2,...,N$, where N denotes the number of cross-sections. Then, without loss of generality, we assume that the height coordinates of the consecutive sections are arranged in ascending order and

$$0 = z_1 < z_2 < ... < z_N = H \ . \tag{3}$$

The values of the profile observed in the subsequent cross-sections are denoted by $r_n^c(\varphi)$. Obviously, measurements performed with the radial method are relative in character, thus

$$r_n^c(\varphi) \cong \rho + r_{cyl}(\varphi, z_n), \ n = 1,2,...,N \tag{4}$$

for an unknown value of ρ . The approximation symbol $\cong$ shows that the measurements of the profile radius contain errors resulting from the measurement noise and the instrument design imperfections. If the coordinates z_n of the cross-sections are uniformly distributed over the range $[0, H]$, then

$$z_n = \frac{H \cdot (n-1)}{N-1}, n = 1,2,...,N \ . \tag{5}$$

Profile measurements at longitudinal sections are performed with the table (spindle) at standstill. A measurement commences after the table is turned to a desired angular position and the vertical sensor shift is switched on. The sensor position can be stabilized by applying an additional run-up section several millimeters in length. It is essential that the height of the sensor after switching on the shift be smaller than the initial height of the analyzed cylindricity profile. Assume that the angular coordinates of the longitudinal sections are: $\varphi_m, m = 1,2,...,M$, where M denotes the number of sections.

The values of the profile at the consecutive longitudinal sections are denoted by:

$$r_m^\ell(z) \cong \rho + r_{cyl}(\varphi_m, z), \ m = 1,2,...,M \ . \tag{6}$$

Additionally, if we assume that the angular coordinates φ_m of the longitudinal sections are uniformly distributed in the range $[0, 2\pi]$, then $\varphi_m = \dfrac{2\pi(m-1)}{M}, m = 1,2,...,M$. (7)

The points of intersection of the scanning trajectories will play an important role in this study. The coordinates are $(\varphi_m, z_n), \quad m = 1,...,M, \ n = 1,...,N$, while the values of the profile radius are:

$$\tilde{r}_{nm}^c = r_n^c(\varphi_m) \ \text{and} \ \ \tilde{r}_{nm}^l = r_m^l(z_n) \ , \tag{8}$$

respectively.

3. THE PROBLEM OF OPTIMAL PROFILE MATCHING

After a cylindricity measurement conducted by means of the bird-cage method, one can observe that the values of the profile radius at the points of intersection of scanning trajectories at the cross and longitudinal sections are slightly different. The difference may be due to the occurrence of measurement noise and instrument vibrations or the design imperfections of the sensor system. Note that the measurement conditions for the cross-section method are different from those for the generatrix method. This causes different distribution of forces acting on the sensor tip. As a result, the profile observed with the cross-section method can be slightly shifted in relation to the profile observed with the generatrix method.

3.1. Comparing the measurement results obtained by the cross-section and the generatrix methods

A profile shift can be best observed in a spatial diagram of measuring points in a cylindrical coordinate system (φ, z, r) . Figure 2 illustrates the results of a series of cylindricity measurements performed on a radial cylindricity measurement instrument. The points obtained by means of the cross-section and the generatrix methods are highlighted in blue and green, respectively. The first five measurements were conducted for rollers with a diameter of 52mm and a height of 100mm, each. The surface preparation involved polishing (the first three specimens) or grounding (the fourth and fifth specimens). There is a clear difference in the waviness level. The rollers were produced for the purposes of the research project No 4 T07D 021 27 financed by the National Committee for Scientific Research. The last three measurements were carried out for rollers with a diameter of 38mm and a height of 62mm, each. Such rollers are used in bearings produced by FŁT Kraśnik S.A.

As can be seen, there is a clear positive shift of straightness profiles in relation to roundness ones. The shift was calculated basing on the radius of the mean cylinder. The calculations were performed separately for the cross-section method and the generatrix method. The values are presented in Table 1. As can be seen, the differences in the mean profile radius range from 0.2 to more than 1.0 μm.
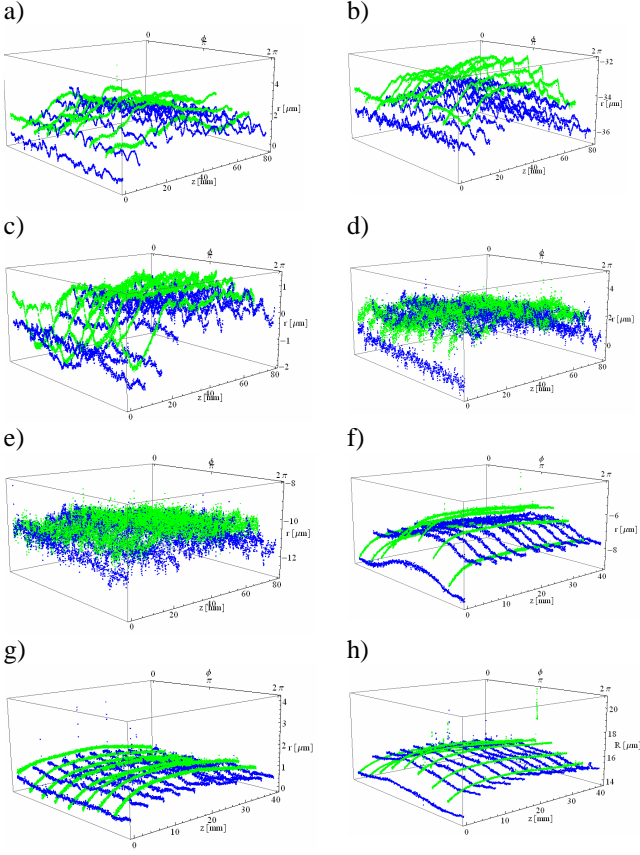
Fig.2. Examples of spatial diagrams of the measuring points in the cylindrical coordinate system

Table 1. Average values of the profiles obtained by means of the cross-section and the generatrix methods - comparison of cross and longitudinal sections

Sample	R_o^c [μm] Cross sections	R_o^ℓ [μm] Longitudinal sections	Difference $R_o^c - R_o^\ell$
a	1.55	2.08	-0.52
b	-34.71	-33.32	-1.38
c	-0.16	0.27	-0.44
d	1.74	2.04	-0.30
e	-10.78	-10.46	-0.32
f	-7.21	-6.91	-0.30
g	0.66	0.90	-0.23
h	15.44	15.86	-0.41

3.2. Formulation and solution of the problem of optimal profile matching

Let us first consider an ideal device with error-free representation of the measured profile $r_{\mathrm{cyl}}(\varphi, z)$. If cylindricity is measured with an ideal instrument using the bird-cage method, we obtain the following set of values of the profile radius:

$$r_n^c(\varphi) = \rho + r_{\mathrm{cyl}}(\varphi, z_n), \quad n = 1,2,...,N, \qquad (9)$$

$$r_m^\ell(z) = \rho + r_{\mathrm{cyl}}(\varphi_m, z), \quad m = 1,2,...,M, \qquad (10)$$

for an unknown value of ρ. In this case, at the points of intersection of profile scanning trajectories, the condition $r_n^c(\varphi_m) = r_m^\ell(z_n)$ is fulfilled. Using the notation of Eq. (8), we have

$$\tilde{r}_{nm}^c = \tilde{r}_{nm}^\ell. \qquad (11)$$

Due to measurement errors, the condition is fulfilled only approximately. Assume, at the first step, that due to the different distribution of forces acting on the sensor tip during roundness and straightness measurements, the difference between the observed radii $\tilde{r}_{nm}^c - \tilde{r}_{nm}^\ell$ at points (φ_m, z_n) is constant. Let us consider, however, a more general case. Assume that the difference between the actual and the observed profiles is different for each cross-section. Thus,

$$r_{nm}^c \cong \rho_n^c + r_{\mathrm{cyl}}(\varphi_m, z_n), \quad n = 1,2,...,N, \ m = 1,2,...,M, \quad (12)$$

$$r_{nm}^\ell \cong \rho_m^\ell + r_{\mathrm{cyl}}(\varphi_m, z_n), \quad n = 1,2,...,N, \ m = 1,2,...,M. \quad (13)$$

for unknown values of ρ_m^c and ρ_n^ℓ. Now, it is essential to calculate the values of ρ_m^c and ρ_n^ℓ so that the error of profile matching $\tilde{r}_{nm}^c - \tilde{r}_{nm}^\ell$ is the smallest possible. Taking into account the above relationships, we obtain:

$$\tilde{r}_{nm}^c - \rho_n^c \cong \tilde{r}_{nm}^\ell - \rho_m^\ell, \quad n = 1,2,...,N, \ m = 1,2,...,M. \quad (14)$$

The number of equations $N \cdot M$ is much bigger than the number of unknown parameters. Furthermore, it should be noted that each measurement signal contains a noise. It is thus reasonable to introduce the index of profile matching:

$$J(\rho_1^c,...,\rho_N^c,\rho_1^\ell,...,\rho_M^\ell) = \frac{1}{2}\sum_{n=1}^{N}\sum_{m=1}^{M}\left(\tilde{r}_{nm}^c - \rho_n^c - \tilde{r}_{nm}^\ell + \rho_m^\ell\right)^2. \quad (15)$$

The values of $\rho_1^c,...,\rho_N^c,\rho_1^\ell,...,\rho_M^\ell$ minimizing the index J are calculated by equating the partial derivatives $\partial J / \partial \rho_n^c$ and $\partial J / \partial \rho_m^\ell$ to zero. It is easy to check that this system of equations has infinitely many solutions. Indeed, if ρ_n^c and ρ_m^ℓ constitute a certain solution to the system of equations, then the values of $\rho_n^c + \varepsilon$ and $\rho_m^\ell + \varepsilon$ for a certain value of ε are also a solution to this system. Without loss of generality, we can assume that the signal shift for the first roundness profile ρ_1^c is equal to zero. Finally, we obtain a system of equations that can be written in the matrix form:

$$\mathbf{A}\,\boldsymbol{\rho} = \mathbf{b}, \qquad (16)$$

where

$$\boldsymbol{\rho} = [\rho_2^c ... \rho_N^c \ \rho_1^\ell ... \rho_M^\ell]^T, \qquad (17)$$

$$\mathbf{A} = \begin{bmatrix} N & 0 & -1 & \cdots & -1 \\ 0 & \ddots & 0 & \vdots & \ddots & \vdots \\ 0 & 0 & N & -1 & \cdots & -1 \\ -1 & \cdots & -1 & M & 0 & 0 \\ \vdots & \ddots & \vdots & 0 & \ddots & 0 \\ -1 & \cdots & -1 & 0 & 0 & M \end{bmatrix} \begin{matrix} \left.\vphantom{\begin{matrix}N\\0\\0\end{matrix}}\right\} N-1 \\ \\ \left.\vphantom{\begin{matrix}N\\0\\0\end{matrix}}\right\} M \end{matrix} , \tag{18}$$

$$\mathbf{b} = \begin{bmatrix} \sum_{m=1}^{M}(\tilde{r}_{2m}^{c} - \tilde{r}_{m2}^{\ell}) \\ \vdots \\ \sum_{m=1}^{M}(\tilde{r}_{Nm}^{c} - \tilde{r}_{mN}^{\ell}) \\ -\sum_{n=1}^{N}(\tilde{r}_{n1}^{c} - \tilde{r}_{1n}^{\ell}) \\ \vdots \\ -\sum_{n=1}^{N}(\tilde{r}_{nM}^{c} - \tilde{r}_{Mn}^{\ell}) \end{bmatrix} . \tag{19}$$

After calculating the values of the parameters ρ_n^c and ρ_m^ℓ, we modify the value of the observed profile in accordance with the formula:

$$r_n^c(\varphi) := r_n^c(\varphi) - \rho_n^c, \quad n = 2,...,N , \tag{20}$$

$$r_m^\ell(z) := r_m^\ell(z) - \rho_m^\ell, \quad m = 1,2,...,M . \tag{21}$$

This approach can be slightly generalized. The axis of rotation in the instruments with a rotary table may be dependent to a certain degree on the rotational velocity of the table (Fig. 3). The position of the axis of rotation may differ if measurements are performed by means of the cross-section method (with the table in rotary motion) and the generatrix method (with the table at standstill). The change in the position of the table rotation axis can be compensated for by modifying the profile according to the following relationship:

$$r_n^c(\varphi) := r_n^c(\varphi) - \rho_n^c, \quad n = 2,...,N , \tag{22}$$

$$r_m^\ell(z) = r_m^\ell(z) - \rho_m^\ell - (\Delta E_x + \Delta D_x z)\cos\varphi_m \\ - (\Delta E_y + \Delta D_y z)\sin\varphi_m, n = 1,2,...,N, m = 1,2,...,M \tag{23}$$

where $\Delta E_x, \Delta D_x, \Delta E_y, \Delta D_y$ are additional parameters defining the reciprocal position of the table axes. Like in the previous case, we assume that $\rho_1^c = 0$. Moreover, the relative eccentricity ΔE_x and ΔE_y can be compensated for by selecting freely the parameters ρ_m^ℓ. We can, therefore, assume that $\Delta E_x = \Delta E_y = 0$. Finally, the parameters responsible for the profile matching are calculated by minimizing the index

$$J(\rho_2^c,...,\rho_N^c,\rho_1^\ell,...,\rho_M^\ell,\Delta D_x,\Delta D_y)$$
$$= \frac{1}{2}\sum_{n=1}^{N}\sum_{m=1}^{M}\left(\tilde{r}_{nm}^c - \rho_n^c - \tilde{r}_{nm}^\ell + \rho_m^\ell + \Delta D_x z_n \cos\varphi_m + \Delta D_y z_n \sin\varphi_m\right)^2, \tag{24}$$

thus

$$\mathbf{A_1 \rho_1 = b_1} , \tag{25}$$

where

$$\rho_1 = [\rho^T \mid \Delta D_x \; \Delta D_y]^T , \tag{26}$$

$$\mathbf{A_1} = \begin{bmatrix} \mathbf{A} & \mathbf{L}^T \\ \mathbf{L} & \mathbf{K} \end{bmatrix} , \tag{27}$$

$$\mathbf{L}^T = \begin{bmatrix} -z_2 \sum_{m=1}^{M}\cos\varphi_m & -z_2 \sum_{m=1}^{M}\sin\varphi_m \\ \vdots & \vdots \\ -z_N \sum_{m=1}^{M}\cos\varphi_m & -z_N \sum_{m=1}^{M}\sin\varphi_m \\ \cos\varphi_1 \sum_{n=1}^{N}z_n & \sin\varphi_1 \sum_{n=1}^{N}z_n \\ \vdots & \vdots \\ \cos\varphi_M \sum_{n=1}^{N}z_n & \sin\varphi_M \sum_{n=1}^{N}z_n \end{bmatrix} , \tag{28}$$

$$\mathbf{K} = \sum_{n=1}^{N} z_n \begin{bmatrix} \sum_{m=1}^{M}\cos^2\varphi_m & \sum_{m=1}^{M}\cos\varphi_m\sin\varphi_m \\ \sum_{m=1}^{M}\cos\varphi_m\sin\varphi_m & \sum_{m=1}^{M}\sin^2\varphi_m \end{bmatrix} , \tag{29}$$

$$\mathbf{b_1} = \begin{bmatrix} \mathbf{b} \\ \hline \sum_{n=1}^{N}\sum_{m=1}^{M}z_n\sin\varphi_m\left(\tilde{r}_{nm}^c - \tilde{r}_{nm}^\ell\right)^2 \\ \sum_{n=1}^{N}\sum_{m=1}^{M}z_n\sin\varphi_m\left(\tilde{r}_{nm}^c - \tilde{r}_{nm}^\ell\right)^2 \end{bmatrix} . \tag{30}$$
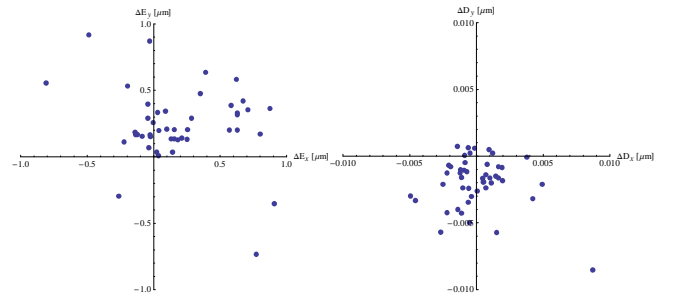
Fig.3. Graphical representation of the difference in the object axis positions determined by means of the cross-section and the generatrix methods: $\Delta E_{x,y} = E_{x,y}^c - E_{x,y}^\ell$ and $\Delta D_{x,y} = D_{x,y}^c - D_{x,y}^\ell$, respectively; the results were obtained for different cylindrically shaped objects.

4. EXPERIMENT

The effects of the application of the profile matching algorithms will be analyzed basing on the measurements of two rollers with a diameter of 52 mm and a height of 100 mm, each. One specimen was polished and the other was ground. The measurements were conducted for the following number of samples and cross-sections:

$N = 11$; $N_c = 2^{10}$, $M_\ell = 2^{11}$, $M = 8$.

The cross and longitudinal sections are distributed uniformly.

4.1. The roller with polished surface

Figure 4 shows a diagram of measuring points in the cylindrical coordinate system. As can be seen, there is a clear positive shift of profiles at the longitudinal sections in relation to those at the cross-sections. The difference is more visible in the point diagram in Fig. 5. where the values of profile radius at the points of intersection of the cross and longitudinal sections are shown. Red lines were drawn between points with the same coordinates (φ_n, z_m) to improve the diagram visibility. The root-mean-square and the arithmetic mean of the difference $\tilde{r}_{nm}^c - \tilde{r}_{nm}^\ell$ were:

$$\Delta R_{QM} \overset{df}{=} \sqrt{\frac{1}{NM}\sum_{n=1}^{N}\sum_{m=1}^{M}\left(\tilde{r}_{nm}^c - \tilde{r}_{nm}^\ell\right)^2} = 1,326, \text{ and}$$

$$\Delta R_{AM} \overset{df}{=} \frac{1}{NM}\sum_{n=1}^{N}\sum_{m=1}^{M}\left(\tilde{r}_{nm}^c - \tilde{r}_{nm}^\ell\right) = -1,286, \text{ respectively.}$$

As we can see, the profile shift exceeds 1µm.
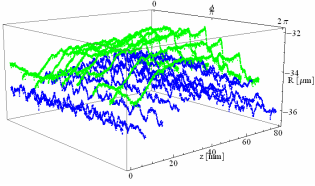
Fig.4. Spatial diagram of the measuring points in the cylindrical coordinate system: surface after polishing
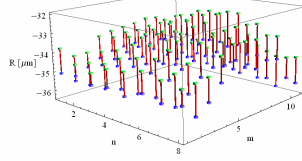
Fig.5. Point diagram of the radius values at the points of intersection of the cross and longitudinal section trajectories

If the algorithm is applied, then the matching parameters are as follows:

$\rho_2^c,...,\rho_N^c$: {-0.56139, -0.170674, -0.477659, -0.398797, -0.447825, -0.52142, -0.360236, -0.337582, -0.235581, -0.437865} [µm],

$\rho_1^\ell,...,\rho_M^\ell$: {0.826792, 0.681831, 0.668199, 0.992521, 1.12382, 1.17622, 1.08581, 0.859522} [µm],

$\Delta D_x, \Delta D_y$: {-0.0021617, -0.001809} [µm/mm].

The root-mean-square and the arithmetic mean of the difference in the radii after matching were:

$$\Delta R_{QM} = 0.08722 \text{ and } \Delta R_{AM} = 0, \text{ respectively.}$$

The results of the optimal matching algorithm are very satisfactory. The root-mean-square of the difference in the radii decreased approximately twentyfold. The zero value of the arithmetic mean is obvious and results from the least squares principle. The next figures show diagrams of the profile after matching, i.e. the diagram in the cylindrical coordinate system, the diagram in the rectangular coordinate system and the point diagram of the radius values at the points of intersection.
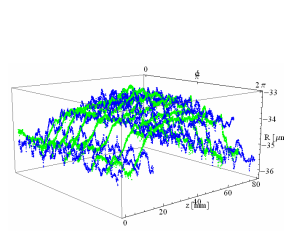
Fig.6. Spatial diagram of measuring points in the cylindrical coordinate system after profile matching
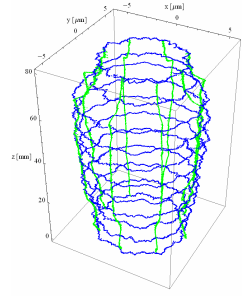
Fig.7. Spatial diagram of measuring points in the rectangular coordinate system after profile matching
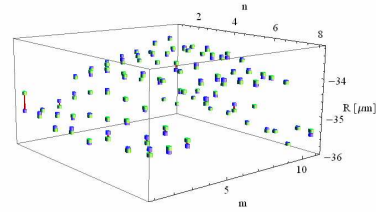
Fig.8. Point diagram of the radius values at the points of intersection of the cross and longitudinal section trajectories after profile matching

4.2. The roller with ground surface

The tests were repeated for the roller with ground surface. The root-mean-square and the arithmetic mean of the difference in the radii $\tilde{r}_{nm}^c - \tilde{r}_{nm}^\ell$ were:

$$\Delta R_{QM} = 0.480425 \text{ and } \Delta R_{AM} = -0.276946,$$

respectively. The profile shift is considerably smaller than in the previous case. This testifies to large randomness of the shift phenomenon. By applying the algorithm, it was possible to obtain the following values of the matching parameters:

$\rho_2^c,...,\rho_N^c$: {0.0763101, 0.452171, -0.334644, 0.0463824, -0.10062, -0.11645, 0.0498365, -0.0082145, 0.0357696, -0.343175} [µm];

$\rho_1^\ell,...,\rho_M^\ell$: {-0.00555966, -0.148586, -0.154116, 0.0255606, 0.418901, 0.519038, 0.796243, 0.587623} [µm],

$\Delta D_x, \Delta D_y$: {-0.000490431, 0.00530184} [µm/mm].

The root-mean-square and the arithmetic mean of the difference in the radii after profile matching were:

$$\Delta R_{QM} = 0.235418 \text{ and } \Delta R_{AM} = 0, \text{ respectively.}$$

As can be seen, the average difference in the radii decreased only twofold. This is due to the occurrence of large profile waviness component. The influence of the waviness on the value of the profile is rather accidental because of the measurement errors such as vibrations or measurement noise. The phenomenon was analyzed thoroughly in Ref. [11].
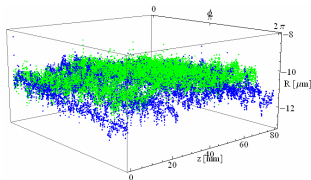
Fig.9. Spatial diagram of the measuring points in the cylindrical coordinate system: surface after grinding
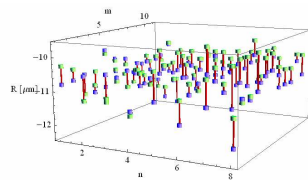
Fig.10. Point diagram of the radius values at the points of intersection of the cross and longitudinal section trajectories
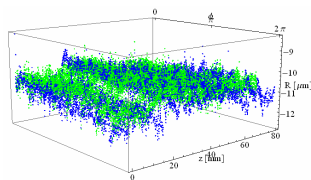
Fig.11. Spatial diagram of the measuring points in the cylindrical coordinate system after profile matching
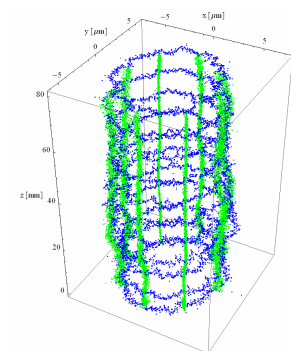
Fig.12. Spatial diagram of the measuring points in the rectangular coordinate system after profile matching
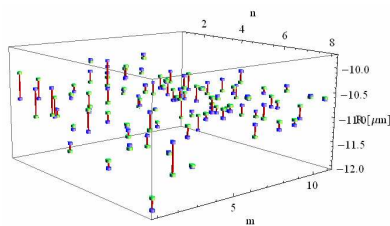
Fig.13. Point diagram of the radius values at the points of intersection of the cross and longitudinal section trajectories after profile matching

5. CONCLUSIONS

The results of the measurements conducted by means of the bird-cage method for various cylindrically shaped objects show a shift in the average values of the profile measured with the cross-section and the generatrix methods. The shift may be up to tenths of the micrometer, and, in extreme cases, more than a micrometer. The shift is probably due to a different distribution of forces acting on the sensor tip during measurements with the cross-section and the genera-

trix methods. To eliminate the errors, it was necessary to formulate and solve the problem of optimal profile matching, which involved shifting the profile values at the consecutive cross-sections in such a way that the difference in the radii at the points of intersection of the scanning trajectories was the smallest possible. Additionally, it was essential to correct the difference in the rotation axis position during roundness measurements with the spindle in rotary motion and during straightness measurements with the spindle at standstill. The results of the experiment show that due to the optimal profile matching, the root-mean-square of the difference in the radii at the points of intersection of the scanning trajectories may decrease from several to several dozen times depending on the level of the waviness component.

REFERENCES

[1] Chou Skuo-Yan, Sun Chung-Wei, "Assessing cylindricity for oblique cylindrical features", *Int. J. of Machine Tools & Manufacture*, vol. 40, pp. 327-341, 2000.

[2] K.D. Summerhays, R.P. Henke, J.M. Balwin, R.M. Casssou, C.W. Brown, "Optimizing discrete point sample patterns and measurement data analysis on cylindrical surfaces with systematic form deviations", *Precision Engineering*, vol. 26, pp. 105-121, 2002.

[3] W. Gao, J. Yokoyama, H. Kojima, S. Kiyono, "Precision measurement of cylinder straightness using a scanning multi-probe system", *Precision Engineering*, vol. 26, pp. 279-288, 2002.

[4] Y.-Z. Lao, H.-W. Leong, F.P. Preparata, G. Singh, "Accurate cylindricity evaluation with axis-estimation preprocessing", *Precision Engineering*, vol. 27, pp. 429-437, 2003.

[5] S. Adamczak, D. Janecki, "A concept of reference measurements of cylindrical machine parts", *Proceedings of the 9th Conference on Metrology in Mechanical Engineering Technologies*, Częstochowa University of Technology, vol. 1, pp. 189-196. Poland, 2001

[6] D.G. Chetwynd, *A unified approach to the measurement analysis of nominally circular and cylindrical surfaces*, Doctoral Thesis, University of Leicester, 1980.

[7] D. Janecki, K. Stępień, "Applying normalized cross correlation function to the comparison of cylindricity profiles", *Metrology and Measurement Systems*, vol. 11, n. 3, pp. 209-220, 2005.

[8] STANDARD: ISO/TS 12180: *Geometrical Product Specifications (GPS) - Cylindricity -* Part 1: Vocabulary and parameters of cylindrical form, Part 2: Specification operators, 2003.

[9] S. Adamczak, D. Janecki, J Świderski, "Combined roundness and straightness measurement applied to the assessment of cylindricity profiles of machine parts", *Pomiary, Automatyka, Kontrola*, n. 5, pp. 248-250, Warsaw 2008.

[10] D. Janecki, S. Adamczak, K. Stępień, "Calculating associated cylinder axis for elements measured by the bird-cage method", pp. 156-160, *9th ISMQ*, Chennai, India, 2007.

[11] S. Adamczak, D. Janecki, R. Domagalski, "Experimental significance of the calculation of harmonic components in roundness and waviness profiles", *Pomiary, Automatyka, Kontrola*, n. 5, pp. 17-20, Warsaw 2000.